

Chapter 2

Recent terrestrial and carbonate fluxes in the pelagic eastern Mediterranean; a comparison between sediment trap and surface sediment*

Abstract – A sediment trap mooring has been deployed in the central eastern Mediterranean from November 1991 to August 1994. At 3000 m water depth, total mass, Al, Ca, Mg, Sr and ^{230}Th fluxes recovered by the sediment trap are highly seasonal, with highest fluxes during early spring in 1992 and 1993, and during late-spring/early-summer in 1994. Comparison of historic annual satellite-derived chlorophyll records with the trap flux time series indicates a lag of 4 to 6 months between maximum primary production in the surface ocean and maximum flux recorded by the trap. Only the flux of coccospheres to the trap is at a maximum ~ 1 month after maximum pigment concentrations in surface waters, a value commonly found in other areas. Quantification of the inorganic (lithogenic) flux to the trap indicates that Saharan dust is likely to be the major contributor to the trap mass flux. The trapping efficiency of the sediment trap, as calculated from the intercepted ^{230}Th flux, is only 23 %, and the trap Al-flux is similarly four times lower than Al fluxes measured in nearby uppermost sediments. Compared with surface sediments, the trap-intercepted carbonate fluxes are even nine times lower than the corresponding lithogenic fluxes. This is partly due to the very low abundance of large (>32 μm) foraminifera and pteropods found in the trap material compared to the surface sediment. We speculate that the period of our sediment trap deployment has been insufficiently long to recover episodic large fluxes, such as may be triggered by variations in the North Atlantic Oscillation.

2.1 Introduction

The eastern Mediterranean Sea is an area that is particularly sensitive to climate change. One expression of this is the recurrent presence of numerous organic carbon rich layers (sapropels; Kidd et al., 1978) in marine cores as well as in marine sections on land, dating back as far as the Miocene (e.g. Cita et al., 1977; Thunell et al., 1977; Kidd et al., 1978; Sigl et al., 1978; Calvert, 1983; Pruyssers et al., 1991; Rohling, 1994; Nijenhuis et al., 1996). The regular occurrence of sapropels has been shown to be related to Milankovitch cycles (e.g. Rossignol-Strick, 1985; Hilgen, 1991; Lourens, 1994). Sapropels are thought to represent periods of high primary productivity and of wet climate (see review by Rohling, 1994) related to maximum Northern Hemisphere insolation caused by a minimum in the Earth's solar precession. At present, during a period of dry climate and close to a precession maximum, the eastern Mediterranean basin is an oligotrophic water body with low primary production. Furthermore, the Saharan desert is an important contributor to the sedimentation

* This chapter has been published as: A. Rutten, G.J. de Lange, P. Ziveri, J. Thomson, P.J.M. van Santvoort, S. Colley and C. Corselli, 2000, *Palaeogeography, Palaeoclimatology, Palaeoecology*, 158, 197–213.

during present time (e.g. Guerzoni et al., 1997, and references therein) due to the prevailing dry climate. However, its contribution is known to strongly decrease during a wet climatic period (e.g. Dominik and Stoffers, 1978). Such alternation leads to variations in the amount and origin of terrestrial matter input into the eastern Mediterranean, which is related to precession cycles.

The overall sedimentation rate in the deep eastern Mediterranean is in the order of $2 - 4 \text{ cm kyr}^{-1}$ (e.g. Thomson et al., 1995; Van Santvoort et al., 1996). Bioturbation causes a mixed depth of 1–2 cm (Thomson et al., 1995), thereby obscuring changes in the sediment flux on yearly and decadal time scales in the geological record. This means that the relation between primary production, climate and seasonal fluxes to the sediment cannot be assessed directly from the sediment record. This relation needs to be better understood so as to obtain insight in the diversity of processes that govern the eastern Mediterranean ecosystem. In addition, this relation is needed for the development of better models for the prediction of the response of the Mediterranean ecosystem to changing climate. One approach to assess seasonal mass fluxes is by using time-series sediment traps.

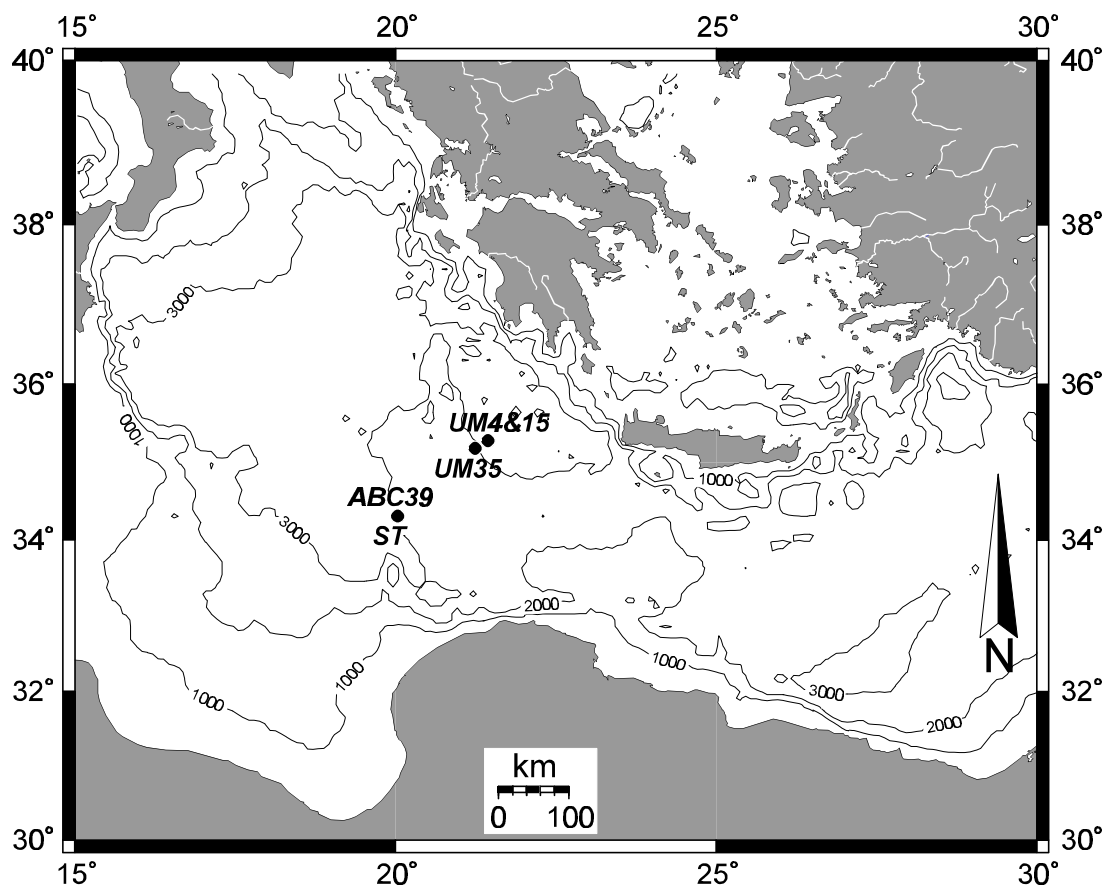


Figure 2.1 Location of the sediment trap (ST) and the boxcores (UM4, UM15, UM35 and ABC39) in the eastern Mediterranean.

A sediment trap deployment was undertaken from November 1991 to August 1994 in the central eastern Mediterranean. In this chapter, we report chemical data on terrestrial and carbonate fluxes, and discuss its relevance in view of seasonal changes. Furthermore, these results will be compared to those estimated from the uppermost sediment of boxcores from nearby sites.

2.2 Materials and methods

2.2.1 Material

2.2.1.1 Sediment trap

Two 1 m² sediment traps (Technicap PPS5/2) were deployed in a time series in the southwestern Bannock Basin (34° 18' N, 20° 01' E; Fig. 2.1). This basin is filled with a brine below 3150 m water depth (Fig. 2.2). The upper trap was located at 3000 meters water depth, well above the sea-water / brine interface in oxygenated conditions, whereas the lower trap at 3500 meters water depth was situated in anoxic brine conditions ~ 20 m above the basin floor (Fig. 2.2). Four time series deployments of 24 samples each were collected in both traps over a nearly continuous period of 34 months (Table 2.1). No preservatives were used in the sample bottles. However, this will not have altered our results significantly (Peterson et al., 1993; Khripounoff and Crassous, 1994). In this study we focus on the upper, oxic trap.

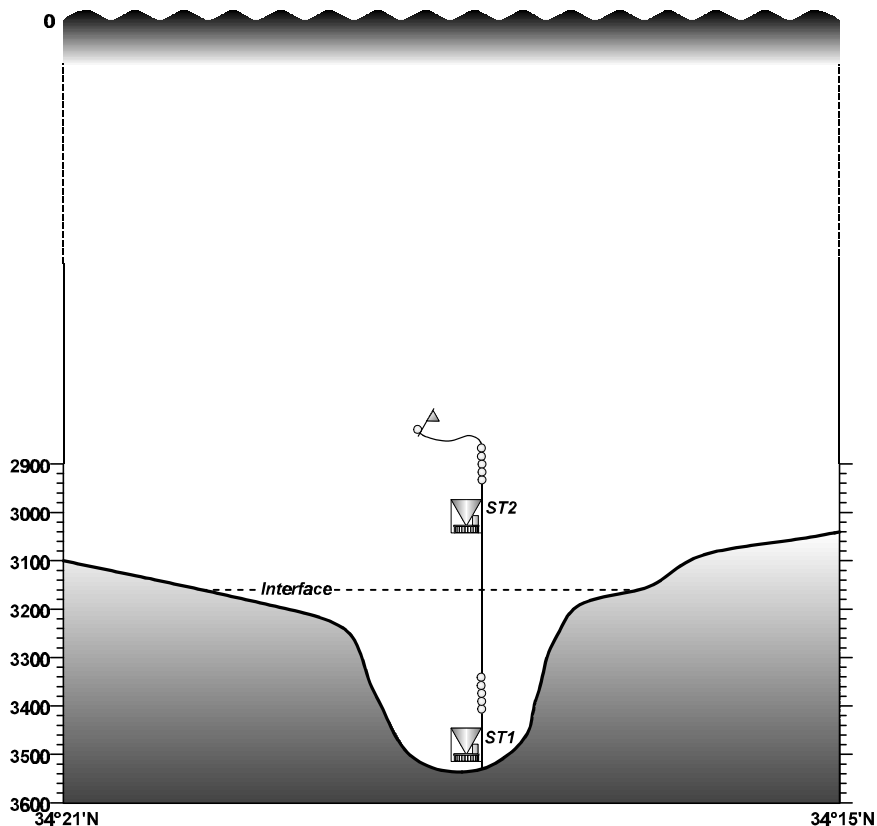


Figure 2.2 Sediment trap mooring in Bannock Basin.

2.2.1.2 Boxcores

The upper few centimetres of three eastern Mediterranean boxcores, from different water depths and located near the sediment trap, were analysed (Fig. 2.1; Table 2.2). The tops of UM4, UM15 and UM35 contained an oxic, light-brown ooze, which overlay a red-brown, oxidised zone. A double manganese peak, indicative of a burn-down front (Thomson et al., 1995; Van Santvoort et al., 1996; Chapters 1, 4, 5), was found in all three cores. Below the oxidised zone, black-green sapropel S1 sediments were found. All boxcores are rich in pteropods and foraminifera throughout. Cores UM15 and UM35 are described in more detail in Van Santvoort et al. (1996). For the analysis of individual pteropods, the top of boxcore ABC39, containing oxic sediment and located close to the sediment trap site, was available.

Table 2.1 *The periods of deployment of the sediment traps (3000 and 3500 m depth) in Bannock Basin (water depth 3520 m). Both sediment traps have the same sampling intervals.*

Mooring	Start date	End date	Deployment (days)	Sample interval (days)
ST2	10 Nov 1991	10 May 1992	182.5	5–10
MT40	1 Jun 1992	19 Feb 1993	263	9–14
MU-B	1 Apr 1993	16 Sep 1993	168	7
UM1STO	20 Oct 1993	29 Aug 1994	313	10–20

2.2.2 Methods

2.2.2.1 Sediment traps

Upon retrieval of the sediment trap, the samples were divided on board into eight aliquots using a pneumatic splitter (Tennant and Baker, 1992). Seven aliquots were filtered using a gas pressure system; four of which were filtered on 0.2 μm cellulose acetate filters, three on 0.8 μm glass fiber filters. The remaining aliquot was either filtered on a cellulose acetate filter or maintained in solution (the last series (UM1STO; Table 2.1) only). All samples were stored at 4°C in air-tight containers until analysis.

For total elemental analysis one cellulose acetate filter was dried at 40°C and weighed. Subsequently, the filter was sealed in a Teflon bomb with 2.5 ml HF and 2.5 ml HClO₄/HNO₃ and dissolved by oven heating at 90°C for 5 hours. The solution was evaporated to dryness and redissolved in 7.5 ml 1 M HCl, and analysed with an inductively coupled plasma atomic emission spectrometer (ICP-AES; Perkin Elmer Optima 3000) for Al, Ca, Mg and Sr. Filter blanks as well as a calibration series of an in-house standard were simultaneously processed and used to calculate separate calibration lines for each element. In Appendix 2-A, the procedure is given in detail.

Table 2.2 Location of the boxcores. ABC39 was recovered during the 1987 cruise of R.V. Tyro, the other three during the 1994 cruise of R.V. Urania.

Boxcore code	Water depth (m)	Latitude	Longitude	Environment
ABC39	2800	34°19.3' N	20°01.6' E	oxic, pelagic
UM4	3309	35°17.30' N	21°24.85' E	oxic, pelagic
UM15	3308	35°17.39' N	21°24.82' E	oxic, pelagic
UM35	2672	35°11.04' N	21°12.54' E	oxic, pelagic

Total mass was determined in two ways, namely from: 1) The difference between the total weight of the filter after drying and the average weight of the filter alone; 2) The total of all elements measured with ICP transferred into oxides (except CaCO₃ and SrCO₃). Both methods give similar results.

Supernatant water was collected immediately after opening the sampling bottles of the sediment trap and stored at 4°C in polyethylene flasks for further analysis. The water samples were diluted eight times for Ca analysis by ICP-AES (Perkin Elmer Optima 3000). The quality of the analyses was monitored by the inclusion of sea water standards.

Current meter (NBA) data were only available for the third (MU-B; Table 2.1) series.

2.2.2.2 Thorium-230 and trap efficiency

Radionuclides were measured on a separate cellulose acetate filter. Due to the small mass of many samples and the low overall levels of radioactivity, a combination of samples was made, such that 39 samples each covering a similar time period were analysed for the natural alpha-emitting uranium and thorium isotopes and ²¹⁰Pb (Colley et al., 1995). Even with the combination of samples, these were demanding low-level radiochemical measurements, and counting times were typically 7 days and frequently longer.

Recent applications of ²³⁰Th data generally involve the assumption that this natural radionuclide provides the best approximation to a constant flux tracer from the ocean to the sediments (Bacon, 1984). ²³⁰Th is continuously produced from the ²³⁴U present in the sea water, and its short residence time in the water column gives rise to a predictable (²³⁰Th_{excess})₀ flux to the underlying sediments which is a linear function of water depth:

$$\text{Flux } (^{230}\text{Th}_{\text{excess}})_0 = \beta \times z = 0.00263 \times z \text{ (dpm cm}^{-2} \text{ kyr}^{-1}) \quad (1)$$

where β is the production rate of ²³⁰Th from the constant ²³⁴U concentration in sea water (Chen et al., 1986) and z is the water column depth in m. For sediment traps, the formula is best used over a long time period (at least a year; Bacon et al., 1985) because of the usual good correlation between the total mass flux and the fluxes of radionuclides in sediment traps (e.g. Fisher et al., 1988; Moore and Dymond, 1988).

2.2.2.3 Boxcores

Dried boxcore subsamples (250 mg) were sealed in Teflon bombs with a mixture of HF, HNO₃, and HClO₄, and oven digested at 90°C. The solution was subsequently evaporated to dryness. Final solutions were made in 1 M HCl and analysed with ICP-AES (Perkin Elmer Optima 3000) for Al, Ca, Mg, and Sr. The quality of the analyses was monitored by the inclusion of in-house and international standards and precisions were always better than 2 %.

The average sedimentation rates for the upper, oxic, interval of boxcores UM4, UM15 and UM35 were calculated by extrapolation from a known time-marker, i.e. the upper Mn peak (average age of 5 kyr; Thomson et al., 1995). Mean porosity was taken into account in each boxcore for the calculation of mass accumulation rates from the sedimentation rate. The following equation was, therefore, used:

$$\text{MAR} = \text{DBD} \times \text{SR} \quad (2)$$

where MAR is the mass accumulation rate (mg cm⁻² yr⁻¹), DBD the dry bulk density (g cm⁻³) and SR the sedimentation rate (cm kyr⁻¹). The dry bulk density was calculated as follows:

$$\text{DBD} = (1 - \text{por}) \times \rho \quad (3)$$

where por is the mean porosity of the upper, oxic interval and ρ is 2.5 g cm⁻³.

For the average composition of each boxcore top, the samples from the upper 1 to 2 cm, i.e. the surface mixed layer (Thomson et al., 1995), were averaged. Part of the top two samples of UM4 were wet-sieved to discriminate fractions smaller and larger than 32 μm . The separate size fractions were analysed the same way as the sediment samples above.

Clean pteropods from the top of boxcore ABC39 were handpicked and divided in 10 – 15 mg samples (4 samples, 3 – 4 pteropods per sample). Each sample was dissolved in 1 M HNO₃. The solutions were analysed with ICP-AES (Perkin Elmer Optima 3000) for Ca and Sr. A blank was included, and ICP analysis was monitored by the inclusion of standards.

2.3 Results

2.3.1 Sediment trap fluxes

The observed particle fluxes for the sediment trap deployments are highly seasonal, varying between 0.28 – 446 mg m⁻² day⁻¹ (Fig. 2.3). Marked peaks occur in April 1992, June – July 1992, April – June 1993, and June – August 1994, and have a magnitude between 42 – 80 mg m⁻² day⁻¹. Small maxima are present in the period between November 1993 and April 1994. The three samples collected between April 20 and May 5 1992 are unusual in that the sampling bottles were all empty, whereas the next sample collected from 5 – 10 May 1992 recorded a large flux of 446 mg m⁻² day⁻¹. These four samples are unlikely to be affected by a technical failure, as the sediment trap's performance registration did not indicate a deviation. In addition, a similar anomalously high flux was recorded in the anoxic trap at the same time, but here the three previous samples do contain sediment. Consequently, this high flux appears to be genuine, and has been included in all calculations.

Individual fluxes of Al, Ca, Mg and Sr show the same trend as the total mass flux

(Fig. 2.3). However, there are subtle differences between biogenic elements such as Ca and Sr on the one hand and terrestrial elements like Al and Mg on the other. In particular, the 1993 flux maximum of Ca and Sr is relatively high compared to those in 1992 and 1994, whereas it is relatively low for Al and Mg.

2.3.2 Thorium-230

The flux of ^{230}Th to the sediment trap is highly seasonal (Fig. 2.3) and correlates linearly with the total mass flux (Fig. 2.4; $r^2 = 0.94$). The slope of the regression line indicates an observed average ^{230}Th concentration of 3.13 dpm/g in the sediment trap samples. The average measured mass flux over the complete deployment of 34 months is $15.9 \text{ mg m}^{-2} \text{ day}^{-1}$ ($0.58 \text{ g cm}^{-2} \text{ kyr}^{-1}$), giving a mean measured ^{230}Th flux of $1.82 \text{ dpm cm}^{-2} \text{ kyr}^{-1}$. The ^{230}Th flux calculated for a trap at 3000 m is $7.89 \text{ dpm cm}^{-2} \text{ kyr}^{-1}$ (using equation (1)). The average sediment trap efficiency is, therefore, 23 %.

2.3.3 Composition of sediment trap samples

The average carbonate content in the sediment trap samples, calculated from total Ca, is 31.5 wt%. Biogenic carbonate is the main carbonate contributor and mostly consists of coccolithophorids, calcareous dinoflagellates and juvenile foraminifers (Ziveri et al., 1995; Chapter 3). Pteropods and large foraminifers, i.e. the coarse fraction, have a notably low abundance. The major component of the mass flux in the sediment trap is lithogenic material (60.4 wt%). This amount was estimated in two ways, namely from: 1) The constant ratio of lithogenic material to Al ($\text{Terr}/\text{Al} = 0.0885$, calculated from the anoxic trap samples); 2) The difference between 'total mass' and the biogenic components (CaCO_3 and organic matter). Both estimates give similar results.

2.3.4 Boxcores

Average total mass fluxes calculated for oxic boxcore tops (UM4, UM15 and UM35) correspond to $85 - 115 \text{ mg m}^{-2} \text{ day}^{-1}$ (Table 2.3). Fluxes of Al and Ca vary between $3.56 - 5.40$ and $17.7 - 23.4 \text{ mg m}^{-2} \text{ day}^{-1}$ respectively. The Ca content, mainly from CaCO_3 , is around 20 wt%, resulting in a carbonate content of ~ 50 wt%. Aluminium concentrations are $4.2 - 4.7$ wt% and are indicative of the lithogenic component.

The size fraction analysis of the topmost sample in oxic boxcore UM4 (0 – 0.5 cm) reveals distinctively different compositions for the two size classes (Table 2.4). The $>32 \mu\text{m}$ fraction contains a high amount of Ca (~ 31 wt%), low Al (~ 2 wt%) and a low Sr/Ca ratio ($\sim 3.2 \text{ mg/g}$), whereas the $<32 \mu\text{m}$ fraction is characterised by a Ca content of ~ 15 wt%, high Al (~ 5.4 wt%) and high Sr/Ca ratios ($\sim 5.5 \text{ mg/g}$). The sample immediately below the topmost sample (0.5 – 1 cm) yielded similar results. The individual analysis of the Sr/Ca ratio of eastern Mediterranean pteropods yields a ratio of $3.60 \pm 0.03 \text{ mg/g}$.

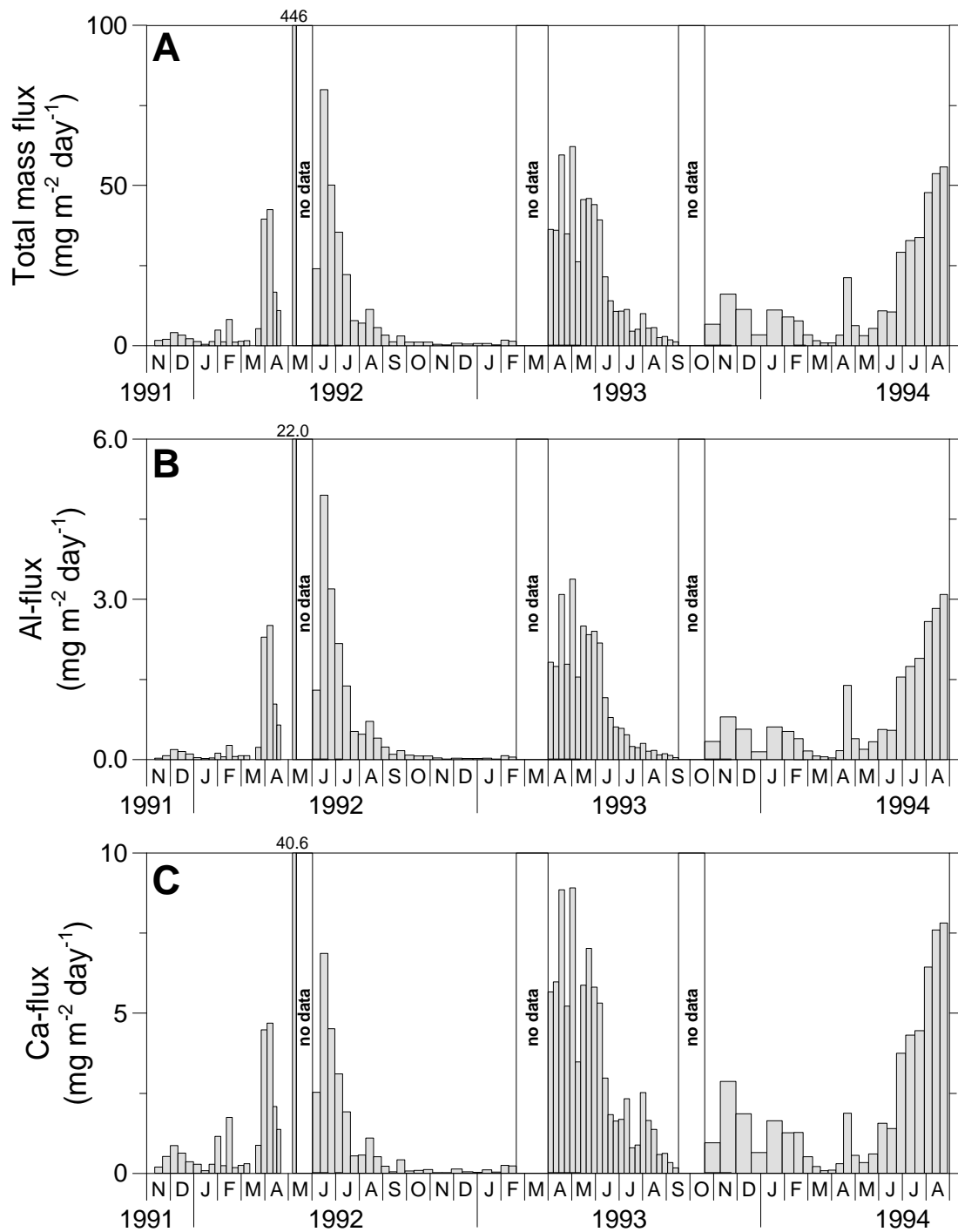


Figure 2.3 Fluxes intercepted during the deployment of the sediment trap in Bannock Basin: A) Total mass flux; B) Al-flux; C) Ca-flux; D) Mg-flux; E) Sr-flux; F) ^{230}Th -flux (including 2σ error bars).

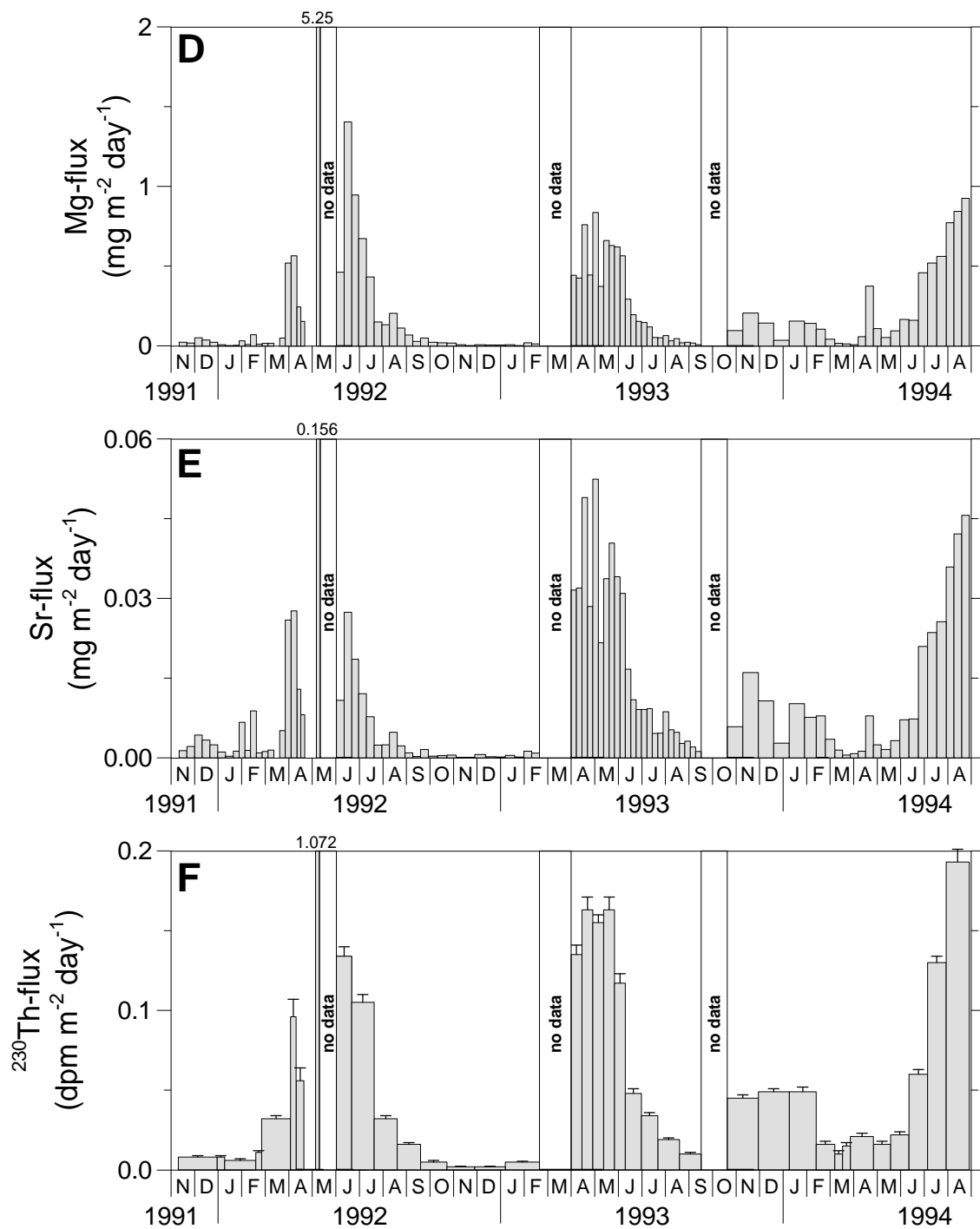


Figure 2.3 (continued)

2.4. Discussion

2.4.1 Seasonal variations recovered in the sediment trap samples

A profound seasonality is recorded in the sediment trap samples recovered between November 1991 and August 1994 (Fig. 2.3). Maximum fluxes occur between April and July in 1992 and 1993, and between June and August (end of the recording period) in 1994. The timing of the flux peaks, therefore, differs per year, as do the flux maxima. The major contributors to the mass flux out of the photic zone appear to be lithogenic material and carbonates (Table 2.5), the latter indicative of primary production, although some carbonate may have a terrestrial origin through the transport of Saharan dust (e.g. Chester et al., 1977; Correggiari et al., 1989). Organic matter and biogenic opal comprise relatively minor fractions. We will now compare the fluxes found in the sediment trap samples with parameters obtained by remote sensing satellite, such as chlorophyll concentrations and desert dust mass.

Table 2.3 Average fluxes and composition of the sediment trap and top sediment samples. The fluxes in the trap have not been corrected for trap efficiency.

	Average flux					Average composition				
	Al	Ca	Mg	Sr	Tot. ^a	Al	Ca	Mg	Sr	Sr/Ca
	(mg m ⁻² day ⁻¹)					(wt%)	(wt%)	(wt%)	(ppm)	(mg/g)
Trap	0.85	2.0	0.23	0.010	15.9	5.37	12.6	1.45	651	5.17
UM4	5.12	21.4	1.73	0.101	109.7	4.67	19.5	1.58	919	4.71
UM15	5.40	23.4	1.98	0.107	114.7	4.71	20.4	1.72	932	4.57
UM35	3.56	17.7	1.41	0.077	85.5	4.17	20.7	1.65	905	4.37

^a Tot. = total mass flux.

Historic satellite-derived chlorophyll data from the Coastal Zone Colour Scanner are only available for the period 1979 – 1985. Data for each month have been averaged for that time period to give the average annual trend (Fig. 2.5). The original chlorophyll data (not shown) indicate that maximum primary productivity occurs, without exception, from December to March, with maximum concentrations in January – February. Although a strong inter-annual variability occurs in the size of the pigment concentrations (indicated by the gray area in Fig. 2.5), the position of the maxima, i.e. mostly January – February, remains the same. Because of this relatively constant behaviour in seasonality of the chlorophyll concentrations, it is justified to compare the seasonality recorded in our sediment trap with the only available, but non-contemporary chlorophyll data. When the timing of the flux

maxima in the sediment trap is compared to that of the pigment data, an average time-lag of 4 to 6 months is apparent. Such a lag is at variance with the sinking rate of particles through the water column usually observed, namely about 100 m day^{-1} (e.g. Neuer et al., 1997, and references therein), which would result in an expected lag of about 30 days. A possible indicator for relatively high primary production is the occurrence of high coccosphere fluxes. A coccosphere represents the complete calcite test of coccolithophores, pelagic unicellular algae that secrete calcite plates (coccoliths). Coccolithophores are the most important primary producers that also manufacture a skeleton in the present-day eastern Mediterranean (Knappertsbusch, 1993; Ziveri et al., 1995; Chapter 3). Maximum fluxes of coccospheres were recorded mostly from January to April (Chapter 3), indicating a time-lag of about 1 month between maximum primary production in the photic zone and its interception at 3000 m water depth. Consequently, the flux of coccospheres appears to be directly linked to the associated surface production. However, the major flux of Ca and individual coccoliths, the latter being three or more orders of magnitude higher than that of coccospheres, occurs at the same time as the main flux of the lithogenic component, i.e. 4 to 6 months after the peak in surface water productivity. The major flux of biogenic particles from the photic zone to the deep water is, therefore, not directly related to primary production.

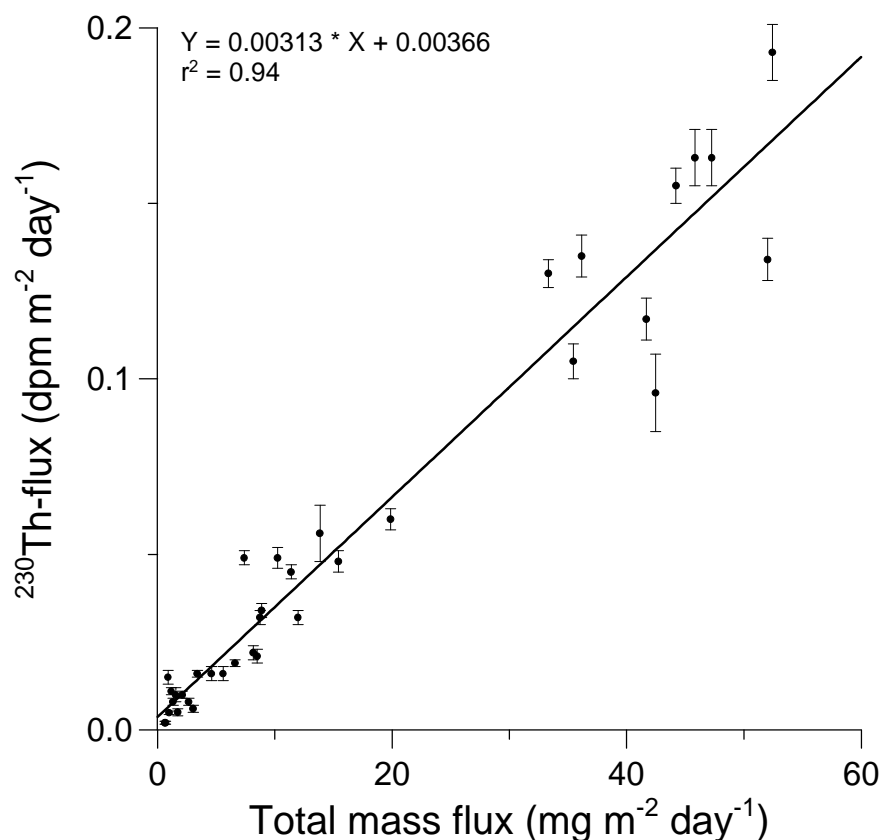


Figure 2.4 Total mass flux vs. ²³⁰Th flux during the sediment trap deployment in Bannock Basin. The vertical error bars designate the error due to counting statistics. The sample collected between 5–10 May 1992 is not shown.

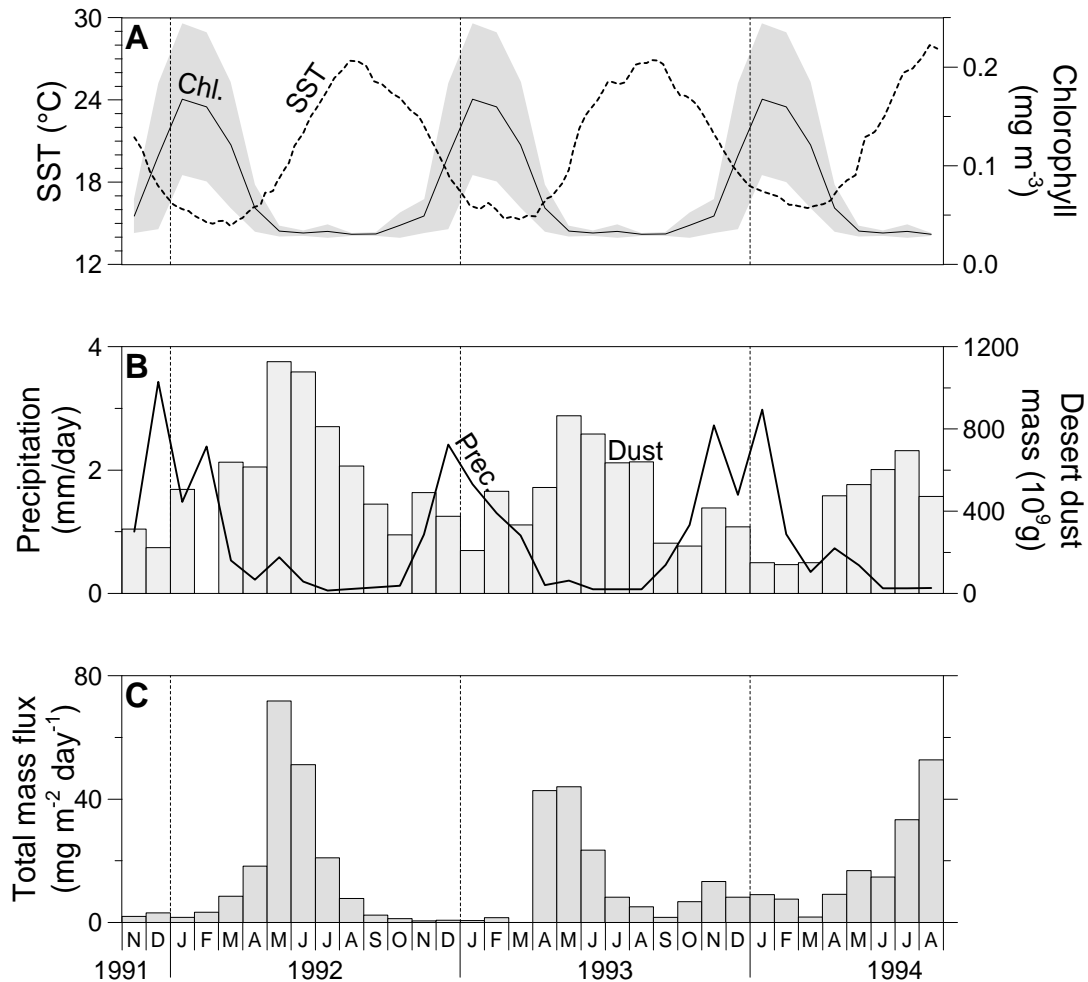


Figure 2.5 Satellite data for the sediment trap location and the monthly averaged total mass flux intercepted by the sediment trap: A) Chlorophyll concentrations (solid line) and sea surface temperature (dashed line). Chlorophyll data were averaged from 1979–1985 monthly CZCS data, with the gray area indicating the 1σ standard deviation for each month. SST data are actual satellite observations made during the deployment period; B) Precipitation and desert dust mass. These are also actual satellite observations made during the deployment period. The dust data were redrawn after Dulac et al. (1996); C) Monthly averaged total mass flux intercepted by the sediment trap. No data were available for March 1993 (see Table 2.1).

Dulac et al. (1996) have derived the monthly desert dust mass above the Mediterranean Sea. Their data indicate that dust concentrations in the atmosphere are high all year long, and at a maximum between May and August (Fig. 2.5). Actual dust deposition is, however, affected by precipitation (Molinaroli et al., 1993), which is high from November to March (Fig. 2.5). Unfortunately, no data are available on actual dust deposition rates in the sediment trap area. Molinaroli et al. (1993) have calculated the dust input into the central Mediterranean (near Sardinia) to be between $0.75 - 1.0 \text{ mg cm}^{-2} \text{ yr}^{-1}$, which has been

corroborated by Guerzoni et al. (1997), who have reported the dust input into the western and eastern Mediterranean Sea to be $1 \text{ mg cm}^{-2} \text{ yr}^{-1}$ and $2 \text{ mg cm}^{-2} \text{ yr}^{-1}$ respectively. When we take the average lithogenic composition of the sediment trap samples (60.4 wt%), the mean total flux of $15.9 \text{ mg m}^{-2} \text{ day}^{-1}$ (Table 2.3) and account for the average trap efficiency of 23 %, then the total detrital flux derived from the sediment trap data is calculated as $1.52 \text{ mg cm}^{-2} \text{ yr}^{-1}$. This flux falls in the range reported by Guerzoni et al. (1997), suggesting that Saharan dust is the most important contributor to the lithogenic material in the sediment trap. We have neglected a possible contribution of rivers to the lithogenic material. A way to estimate the relative contributions of riverine and dust lithogenic material is by making use of the Ti/Al ratio. For rivers, this ratio is reported to be between 48.2 and 59.6 mg/g (Gordeyev and Lisitsyn, 1978; Martin and Meybeck, 1979), whereas dust has a ratio between 57.8 and 69.6 mg/g (Bonelli et al., 1996; Güllü et al., 1996). The average Ti/Al ratio of the sediment trap samples is 68.0 mg/g, also pointing to dust as the major contributor to the lithogenic fraction.

The high fluxes of biogenic and terrigenous material to the sediment trap at 3000 m are coincidental, with a time-lag of 4–6 months after maximum primary production. In most sediment trap studies, the interception of these two types of material is found to occur at the same time (e.g. Honjo et al., 1982; Ramaswamy et al., 1991; Neuer et al., 1997). This relation is established by the incorporation of biogenic as well as lithogenic material in faecal pellets. These sink very fast compared to small particles like coccoliths and clay minerals, which can remain in suspension for long time periods (Lal, 1977; Buat-Ménard et al., 1989). We have found no data on faecal pellet fluxes in the eastern Mediterranean, but in the western Mediterranean, zooplankton grazing activity, resulting in faecal pellet production, was inferred to be mostly responsible for the sedimentation of terrigenous iron (Quérel et al., 1993). This grazing activity was particularly intense from April to June, the same period in which we find the highest mass fluxes in the sediment trap in 1992 and 1993. This might, therefore, explain the co-sedimentation of biogenic and terrigenous particles in this particular period.

The satellite data (Fig. 2.5) indicate that pigment concentrations are highest when sea surface temperature (SST) is lowest. The latter indicates a wind-induced oceanographic change from a summer stratified upper water mass to a deep winter mixing (Krom et al., 1992). This results in the fertilisation of the photic zone, important because the eastern Mediterranean is nutrient-depleted and phosphorus-limited (Zohary and Robarts, 1998). However, dust deposition, mainly occurring in the same period, might also contribute to higher P concentrations in the upper water column. Bergametti et al. (1992) found that the atmospheric input of phosphorus could be significant to northwestern Mediterranean surface waters, especially in summer.

2.4.2 Comparison between trap and sediment

2.4.2.1 Efficiency of the sediment trap

To compare fluxes recorded in a sediment trap with those of surface sediments, it has to be established first whether the flux is efficiently trapped. A widely used method is that by applying ^{230}Th (see section 2.2.2.2). The calculated value of 23 % is extremely low when compared to other sediment trap studies (Anderson et al., 1983a; Bacon et al., 1985; Fisher et al., 1988; Colley et al., 1995). The low efficiency may be the result of three phenomena, namely 1. Boundary scavenging; 2. A water column with unusually low U concentrations; and 3. High current velocities.

Boundary scavenging, i.e. lateral export of ^{230}Th away from the water column above the sediment trap, has not been accounted for in the model calculation. Comparison of ^{230}Th and ^{231}Pa inventories in pelagic as well as near-coastal traps and sediments has shown that a net export of these radionuclides out of the pelagic realm to the ocean boundaries must occur (e.g. Kadko, 1980; Anderson et al., 1983a,b). Because of the pelagic location of our sediment trap, this might also happen at the Bannock site. However, to the best of our knowledge, no ^{231}Pa data for eastern Mediterranean sediments have yet been published. Therefore, no quantification of this boundary scavenging effect can be made. Kadko (1980) found an average of 30 % deficit of $^{230}\text{Th}_{\text{excess}}$ in deep open ocean sediments. This value can, therefore, not fully explain the observed deficit of 77 % in our sediment trap samples (see also next section).

A much lower concentration of ^{234}U in the Mediterranean water column relative to the open ocean might also result in lower ^{230}Th fluxes to the sediment trap. This, however, is ruled out by the long residence time and stability of dissolved U in sea water. Furthermore, the actual U concentration is even slightly higher than average sea water just above the Bannock brine interface (Van der Weijden et al., 1990).

The occurrence of high current velocities would seriously hamper the collection of particles. However, the current meter data from the third (MU-B; Table 2.1) series indicate low velocities, mostly below the detection limit of 1 cm s^{-1} . Speeds were never higher than 7 cm s^{-1} . In addition, the tilt meter mounted on the sediment trap indicates no deviations from the vertical during the sampling period. Consequently, hydrodynamic biases were negligible for the particle flux data (Baker et al., 1988; Gust et al., 1992).

Overviewing these three influencing factors, we believe that only boundary scavenging, if similar to the open ocean, may explain part of the low trapping efficiency as calculated by the ^{230}Th method. Because we cannot quantify this process on the basis of ^{230}Th trap data alone, we will compare fluxes between the sediment trap and top sediment in the following section.

2.4.2.2 Comparison of fluxes and composition

Obviously, average mass fluxes are much lower in the sediment trap samples than in surface sediments (Table 2.3). We will compare the fluxes in the sediment trap with those found in boxcores UM4, UM15 and UM35. These boxcores are not in the immediate vicinity of the sediment trap location. However, a gravity core taken in Bannock Basin, containing

Table 2.4 Composition of the two top samples of boxcore UM4. A part of the sample was sieved to gain two size fractions, which were analysed together with an unsieved sample.

UM4: upper 0.5 cm				
Component	<32 μ m	>32 μ m	total ^a	calc/tot ^b
Al (wt%)	5.41	1.99	4.50	1.00
Ca (wt%)	15.8	31.1	19.6	1.01
Mg (wt%)	1.95	0.72	1.54	1.05
Sr (ppm)	875	1000	923	0.98
Sr/Ca (mg/g)	5.55	3.21	4.72	0.97

^a analysis of the total sample.

^b calculated total (from the two fractions by using the weight fraction) divided by the measured total; weight fraction used: >32 μ m = 0.265.

oxic top sediments and sapropel S1 (GC17; Van Os et al., 1991), has a sediment composition and an accumulation rate comparable to that in UM35. Therefore, a comparison between the oxic boxcores and the sediment trap is justified. We will mainly concentrate on the fluxes in UM35 because of the similar accumulation rate compared to sediments near the trap location.

The Al flux in the sediment trap is about four times lower than it is in UM35 (0.85 vs. 3.56 mg m⁻² day⁻¹), which is close to the estimated trap efficiency of 23 %. This similarity indicates that boundary scavenging of ²³⁰Th is not significant and that the estimated trap efficiency is reliable. Because current velocities are low and tilt meter data show no offset from the vertical, we think that the low sediment trap efficiency cannot be caused by either hydrodynamic bias or boundary scavenging of ²³⁰Th. A possible alternate explanation which may be significant for these low mass fluxes, is the sticking of settling particles to the inner cone of the trap.

The fluxes of Ca, Mg and Sr in the sediment trap are relatively even lower when compared to the surface sediment samples. For Ca, this factor is ~ 9, for Mg ~ 6, and for Sr ~ 8. In the eastern Mediterranean, Ca and Sr reside almost exclusively in the carbonate fraction, whereas Mg is found in both clay minerals (i.e. the lithogenic fraction) and carbonates (Chapters 5 and 7). Aluminium is indicative for clay minerals. The magnitude of the flux and the correlation of Al with other terrigenous elements (K, Ti) must dominate any biogenic scavenging of Al as found by Murray and Leinen (1996) in the central equatorial Pacific Ocean. Consequently, variations in Al content cannot be related to variations in biogenic scavenging but rather to changes in terrigenous input alone. It appears, therefore, that the carbonate component of the total flux is relatively more undertrapped than the terrigenous one. From the faunal and floral analysis of the sediment trap samples, it is clear that the large biogenic carbonate particles, i.e. pteropods and large foraminifers, are rare (Chapter 3), whereas they are common in surface sediments of the eastern Mediterranean. To

investigate this geochemically, two size fractions of surface sediment from UM4, namely one (<32 μm) containing the small biogenic fraction (e.g. coccoliths, calcareous dinocysts, juvenile foraminifers) and the other (>32 μm) including large biogenic particles (foraminifers and pteropods), were analysed. The results indicate that the fine fraction contains only half as much Ca (16 wt%) as the large fraction (30 wt%; Table 2.4). The Sr/Ca values in the fine fraction are distinctly higher than they are in the coarse fraction. Although higher Sr/Ca values are often interpreted to be due to enhanced pteropod contents (Winland, 1969; Sutherland et al., 1984), Krinsley and Bieri (1959) observed a relatively low average Sr/Ca of 2.5 mg/g for eastern Mediterranean pteropods from plankton tows as well as surface sediment. We have also analysed pteropods from the top of a nearby boxcore, and have found a Sr/Ca ratio of 3.60 ± 0.03 mg/g. The latter Sr/Ca ratio is comparable to the one found in our coarse sediment fraction. In contrast, the sediment trap samples have a much higher Sr/Ca ratio, namely 5.2 mg/g, close to that of the fine surface sediment fraction (5.5 mg/g) (compare Tables 3 and 4). All evidence given above, therefore, is consistent with the scarcity of the coarse carbonate fraction in the sediment trap samples. At this moment, however, it is not clear why this fraction is absent in the trap. Hydrodynamic bias in trapping, if at all present, would be expected to lead to a greater loss of smaller particles rather than larger ones. Dissolution can also be ruled out; coccoliths, even delicate forms, are well preserved (Chapter 3), and the Ca concentration of the supernatant water in sediment trap sampling bottles is similar to the sea water value. The observed deviation might arise from the distribution of the coarse size fraction of biogenic carbonate through time. As juvenile foraminifers are always present in the trap samples, the distribution of the large foraminifers and pteropods could be highly variable in time and in place. The resulting magnitude of fluxes at one site may, therefore, have varied over the course of time. A bloom associated with a major hydrodynamic or atmospheric event, and occurring, for example, once every ten years has a large probability of not being trapped during a three-year deployment. An example of such a phenomenon was reported at the Cap Blanc sediment trap site, off the coast of Northwest Africa (Wefer and Fischer, 1993). In a single sampling interval of 17 days, out of three years, an extremely high flux was recorded in the >1 mm size fraction. This fraction contained a monospecific assemblage of pteropods (Kalberer et al., 1993). Another example is a sediment trap study conducted during more than 19 years in the deep Sargasso Sea, which exhibited an episodic occurrence of large, short-lived flux maxima that are not associated with the annual spring bloom in that area and do not necessarily occur every year (Conte et al., 1998). A phenomenon, similar to the ones at Cap Blanc or in the Sargasso Sea, and possibly related to North Atlantic Oscillation (NAO), might occur in the usually low-productive eastern Mediterranean. Moulin et al. (1997) have shown that atmospheric export of Saharan dust to the Mediterranean and North Atlantic Ocean is controlled by NAO. Clearly, long time series sediment trap sampling is needed so as to fully understand the dynamics of seasonal and annual variations in the eastern Mediterranean biogeochemical fluxes.

We will now evaluate if an additional (coarse) fraction in the sediment trap samples might explain the difference between sediment trap and surface sediments. When such a coarse fraction, containing 31.1 wt% Ca (i.e. 77.7 wt% CaCO_3) and having a weight fraction

of 0.265 (as found in the uppermost sample of UM4 (Table 2.4)), is added to the average sediment in the trap, the CaCO_3 content would rise to 43.7 wt%, much closer to the concentrations found in the oxic boxcores (Table 2.5). The CaCO_3 flux would, when including the trap efficiency correction, increase to $41.0 \text{ mg m}^{-2} \text{ day}^{-1}$. This flux is still lower than that found in the oxic boxcore tops, although close to the Ca-flux in UM35 (Table 2.5), possibly reflecting subtle differences in the primary production in the photic zone, hence export production, at the different locations (e.g. sediment trap site vs. UM35 or UM4/UM15 site).

We have related the lithogenic flux in the trap to the input of Saharan dust. For UM35, the lithogenic flux is $1.48 \text{ mg cm}^{-2} \text{ yr}^{-1}$, and for UM4 and UM15 $2.01 \text{ mg cm}^{-2} \text{ yr}^{-1}$. These values are in the same range as those reported by Guerzoni et al. (1997), discussed earlier. Therefore, the sediment trap and boxcore samples are both consistent with the notion that Saharan dust input is the major source for lithogenic matter in this region at present.

Table 2.5 Observed and recalculated total, carbonate and lithogenic fluxes, and composition, for the sediment trap. Organic matter and biogenic opal, the other two contributors to the total mass flux, are not shown. Observed fluxes and composition for the three normal 'oxic' boxcores (UM4, UM15 and UM35) are also listed.

	Flux ($\text{mg m}^{-2} \text{ day}^{-1}$)					
	Trap	Trap*	Trap**	UM4	UM15	UM35
Total	15.9	68.9	93.8	109.7	114.7	85.5
Carbonate	5.0	21.7	41.0	53.4	58.4	44.2
Lithogenic	9.6	41.6	47.5	55.2	55.1	40.6

	Composition (wt%)					
	Trap	Trap*	Trap**	UM4	UM15	UM35
Carbonate	31.5	31.5	43.7	48.7	50.9	52.7
Lithogenic	60.4	60.4	50.6	50.3	48.1	47.4

* Numbers corrected for a sediment trap efficiency of 23 %. Possible lateral export of ^{230}Th is neglected.

** Numbers also corrected by adding a coarse fraction (26.5 wt%) having a composition comparable to that found for the uppermost sample ($>32 \mu\text{m}$) of UM4.

2.5 Conclusions

The total flux of suspended material out of the photic zone to the deep water is low and highly seasonal in the pelagic eastern Mediterranean. The coccosphere-indicated primary productivity maximum reaches the trap about one month after the satellite-inferred chlorophyll maximum. However, the major sediment flux, containing a lithogenic as well as a biogenic fraction (the latter comprised mainly of coccoliths), does not coincide with the coccosphere flux, but rather is recorded 4 to 6 months later, probably due to intense zooplankton grazing, resulting in high faecal pellet production, from April to June. Because coccoliths and clay minerals, comprising most of the biogenic and lithogenic material respectively, can remain in suspension for a long time, they are scavenged and quickly transported by faecal pellets. Quantification of the lithogenic flux indicates that desert dust is likely to be the major component of the detrital matter. The Th-230 based trap efficiency is low (23 %), but is substantiated by the four times lower Al flux of samples in the sediment trap compared to those in boxcore top sediments. Boundary scavenging of ^{230}Th , the most common factor determining the trapping efficiency of ^{230}Th is, therefore, unlikely to be the major cause for the low trap efficiency. Due to the absence of hydrodynamic bias, sticking of settling particles to the inner cone of the sediment trap might have significant influence on the low mass flux. The relative recovery of carbonate in samples from the trap compared to those in the sediment is even lower (1/9). The near absence of the coarse carbonate fraction consisting of large foraminifers and pteropods in the trap samples, compared to their abundant occurrence in top sediment samples, may account for most of this deficiency. Episodically occurring major blooms may have resulted in brief intervals of major coarse carbonate (large foraminifers and pteropods) fluxes that have not been recorded during the time period of our sediment sampling (i.e. from November 1991 to August 1994) and are possibly related to NAO. Clearly, long time series sediment trap observations are needed for this area that is sensitive for recording subtle global climatic variations, so as to fully understand the dynamics of seasonal and annual variations.

Acknowledgements – G. Nobbe and H. de Waard are thanked for their analytical assistance. The pigment data are courtesy of the Joint Research Centre (European Commission / European Space Agency). The SST data were extracted from the Weekly NCEP SST Database at the NOAA/WRC Server Ferret and the precipitation data from the GPCP Global Combined Precipitation Dataset (part of the Climatology Interdisciplinary Data Collection). This chapter greatly benefited from the comments of two anonymous reviewers.

This study was supported by MARFLUX (MAST1-90022C), PALAEOFLUX (MAS2-CT93-0051) and SAP (MAS3-CT97-0137) European programmes.

This is Netherlands Sedimentary Research School (NSG) contribution 990402.

Appendix 2-A: Determination of the inorganic composition, including silica, using total digestion on sediment trap samples

Sediment trap samples, especially those from the oxic trap in the oligotrophic open eastern Mediterranean, are too small to perform separate analyses for total silica and for other major and minor elements by traditional ICP-AES techniques. In the latter preparation, a HF/acid mix total digestion is followed by evaporation of the acids, and the subsequent dissolution in 1 M HCl. During the evaporation step, however, silica is removed as volatile Si fluorides. In addition, routinely such total digestions prior to ICP-AES analyses are done on one 250 mg of sample, whereas the one eighth (aimed for inorganic geochemical analysis) sediment trap samples mentioned above frequently were only a few mg in size.

In this appendix, a method is described to obtain the conventional ICP-AES determined element concentrations as well as the total Si concentration using a single total digestion.

In brief

The sediment trap samples had originally been filtered on board ship, using cellulose acetate filters. In the home laboratory these samples were dried at 40°C in an oven or were freeze-dried. The samples including the filter were then added to a Teflon vessel. A calibration series of MM91, an in-house standard, was also weighed into separate vessels (2, 4, 8, 16, 32, 64, 128 mg). A fresh cellulose acetate filter was added to make the matrix uniform to that of the sediment trap samples. Also, three 'blanks', containing only a cellulose acetate filter, were run. To all these vessels 2.5 ml HF and 2.5 ml mixed acid (60 vol% HClO₄, 30 vol% HNO₃ and 10 vol% distilled water) were added and the closed vessels were put in an oven at 95°C for 5 hours. After cooling down, 200 µl of the HF/mixed acid solution was transferred to a pre-cleaned polyethylene vial already containing 10 ml Milli-Q water. This subsample is subsequently used for the spectrophotometric determination of total Si. The (open) vessels with the remaining 4.8 ml of fluid were then put upon a sand bath at 240°C and the solution was vaporised to near-dryness. The remaining material was redissolved in 7.5 ml 1 M HCl and analysed by Inductively Coupled Plasma Atomic Emission Spectrometry (ICP-AES). The MM91 calibration series was used to calculate separate calibration lines for each element.

In detail

1. Freeze-dry the filter containing the sediment trap sample.
2. Weigh Teflon vessel (small format; 25 ml) including the lid.
3. Weigh filter containing the sediment trap sample.
4. Add the filter containing the sediment trap sample to the Teflon vessel.
5. Weigh Teflon vessel + lid → extra check on the filter+sample weight.
6. Add 2.5 ml HF and 2.5 ml HNO₃/HClO₄ to the Teflon vessel.
7. Put the lid firmly on the Teflon vessel and weigh it → weight of HF+HNO₃/HClO₄ is now known.

8. Put the Teflon vessel for 5 hours in an oven at 95°C.
9. Weigh polyethylene vial including closing cap.
10. Fill vial with 10 ml Milli-Q water and put cap on vial.
11. Weigh filled vial → weight of 10 ml Milli-Q water is now known.
12. Take the Teflon vessel after the 5 hours heating out of the oven, let it cool down, and weigh (to check for possible loss).
13. Unscrew cap and put 200 µl of the solution into the vial containing Milli-Q water.
14. Evaporate the remaining solution in the Teflon vessel to near-dryness.
15. Weigh the closed vial → the weight of 200 µl HF+HNO₃/HClO₄ is now known.
16. Add 7.5 ml 1 M HCl to the Teflon vessel, close the vessel and put it for 2 hours in an oven at 95°C.
17. After 5 hours heating, the Teflon vessel is removed from the oven and cooled down.
18. Weigh the Teflon vessel → the weight of the 7.5 ml 1 M HCl solution (thus including the dissolved elements) is now known.
19. Put the solution into a polyethylene vial for measurement with ICP-AES.

The polyethylene vial containing 10 ml Milli-Q water + 200 µl HF+HNO₃/HClO₄ is used for the spectrophotometric determination of Si.

Notes:

- 1) Steps 9 to 11 and step 13 are meant for the determination of Si.
- 2) The repeated weighing is essential for the calculation of dilution factors.

The spectrophotometric measurement of silica

Total silica content can be reliably determined by the following method using a small subsample of the hydrofluoric/mixed acid mixture. The basic solution is a 50 times diluted acid/sample mixture (200 µl in 10 ml Milli-Q water). Prior to evaporation, no silica will have been removed from solution by the HF reagent. However, the presence of HF in the solution does imply that certain precautions have to be taken (such as for safety, always work in a well-ventilated fume-hood and always wear plastic gloves; do not use glassware anywhere in the procedure, and certainly not glass cuvettes!!).

Reagents

- **MOLYBDATE REAGENT (AMMO):** Dissolve 4 g of ammonium paramolybdate, (NH₄)₆MO₇O₂₄·4H₂O (preferably fine crystalline), in ~ 300 ml Milli-Q water using a 500 ml plastic volumetric flask. Add 12 ml concentrated hydrochloric acid (12 N), mix, and make up the volume to 500 ml with Milli-Q water. This reagent is colourless and is stable for many months if stored in a dark bottle. The reagent should be discarded immediately when any white precipitate forms. If unable to store properly, or if time permits, make fresh for each run.

- **METOL SULPHITE SOLUTION (METOL):** Dissolve 6.0 g anhydrous sodium sulphite, Na_2SO_3 , in a 500 ml plastic volumetric flask. Add 10 g Metol (p-methylaminophenol sulphate) and then Milli-Q water to make the volume to 500 ml. When the metol has dissolved, filter the solution through a Whatman no. 1 filter paper and store in a clean, dark, polyethylene bottle, which is tightly stoppered in the refrigerator. This solution may deteriorate quite rapidly and erratically so it should be prepared fresh every month.
- **OXALIC ACID SOLUTION (OXAL):** Prepare a saturated oxalic acid solution by shaking 50 g of analytical-grade oxalic acid dihydrate, $(\text{COOH})_2 \cdot 2\text{H}_2\text{O}$, with 500 ml of Milli-Q water. Let stand overnight. Decant solution from crystals before use. This solution is stable and can be stored in a polyethylene bottle.
- **SULPHURIC ACID SOLUTION (SULF):** 50% V/V. Using a 500 ml plastic volumetric flask, pour 250 ml concentrated analytical-grade sulphuric acid into ~ 200 ml Milli-Q water. Cool to room temperature and bring volume to 500 ml with a little extra Milli-Q water. Store in a polyethylene bottle.

Standards

A standard series with the following Si concentrations was used for calibration:

0; 6.25; 12.5; 25; 50; 100; 200; 300; 400; 600; 800; 1600; 2600 μM .

To 50 ml of each standard solution, 1 ml of HF/mixed acid was added to assure a matrix similar to that of the samples. All standards were measured in duplicate.

Preparation of reducing solution (RED)

Mix 50 ml METOL with 30 ml OXAL. Add slowly, with mixing, 30 ml SULF and bring volume to 150 ml with Milli-Q water. This solution should be made daily, just before using it.

Method for the silica measurements

1. First, make sure that all reagents are prepared ahead of time. The method has a time factor built in, and therefore it is of great importance to have all necessary reagents ready to go.
2. Label and set up 4.5 ml polystyrene cuvettes (4 clear sides).
3. Put 1.400 ml Milli-Q water into the cuvettes.
4. Add 0.100 ml of sample, standard, or blank, and mix.
5. Record time.
6. Add 1.000 ml of AMMO, and mix. A yellow colour will develop, and this is allowed to mature for exactly 15 minutes (± 15 seconds). Then add 1.50 ml of RED, and mix again. Cover the cuvettes with Parafilm and wait for at least 4 hours.
7. Read absorbances on the Perkin Elmer Lambda 1 UV/VIS Spectrophotometer at 812 nm.

Typical calibration line for Si-standard

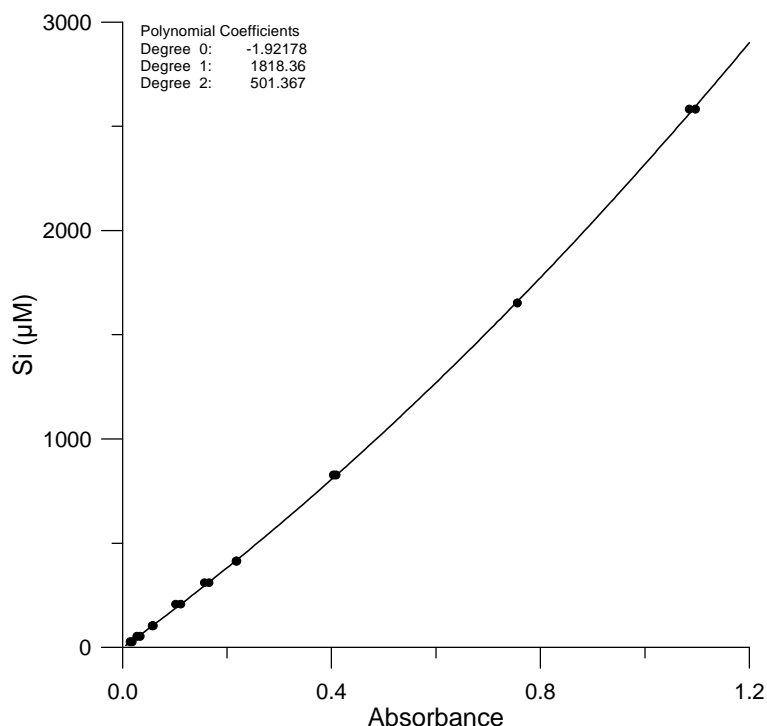


Figure 2-A.1 A typical calibration line for the Si-standard. The absorbance of the Si-standard samples is plotted against the known Si concentration. This calibration line is then used to calculate concentrations from the absorbances of the sediment trap samples and the MM91 calibration series.

Calculation of the Si content of the sediment trap samples

The first step consists of plotting the absorbance of the Si-standard calibration series against the Si concentration of the original solution (Fig. 2-A.1 shows the calibration line from the UM-series of the oxic trap). From this plot a calibration line can be calculated, so as to transform the measured absorbances of the sample solutions into the concentration of the 10 ml Milli-Q water + 200 µl HF/mixed acid. Using the previously measured weights, the amount (in mg) of Si in total HF/mixed acid can be calculated. Then, the measured Si amounts of the MM91 standards are plotted against the expected Si amounts, which are calculated by using the weight of the samples and the known Si content (13.13 wt%) (Fig. 2-A.2 shows the MM91 calibration for the UM series of the oxic trap). The measured Si amount of the sediment trap samples is then transformed into standard-calibrated values so as to avoid procedural artifacts. These Si amounts can be recalculated as Si fluxes. Note: the absorbances of the MM91 calibration series and the sediment trap samples are in the full range of the Si calibration line.

Procedural notes

- Do not handle more than about 60 samples at a time in order to ensure that the 15-minute time limit can be adhered to. Make sure that there are no wild fluctuations in room temperature.
- Although it is suggested that strict adherence to the 15-minute time limit is advisable, tests have shown that there is some leeway, i.e. the yellow molybdate complex is stable from 10 to 20 minutes. However, consistency in the time limit will eliminate any potential error.
- It is important to wait at least 3 hours for the blue colour to develop; the higher the concentration, the longer the time. The colour remains stable for many more hours, and reading after 4 or 5 hours may, in fact, be a good idea. Again, consistency in time limits is advisable.

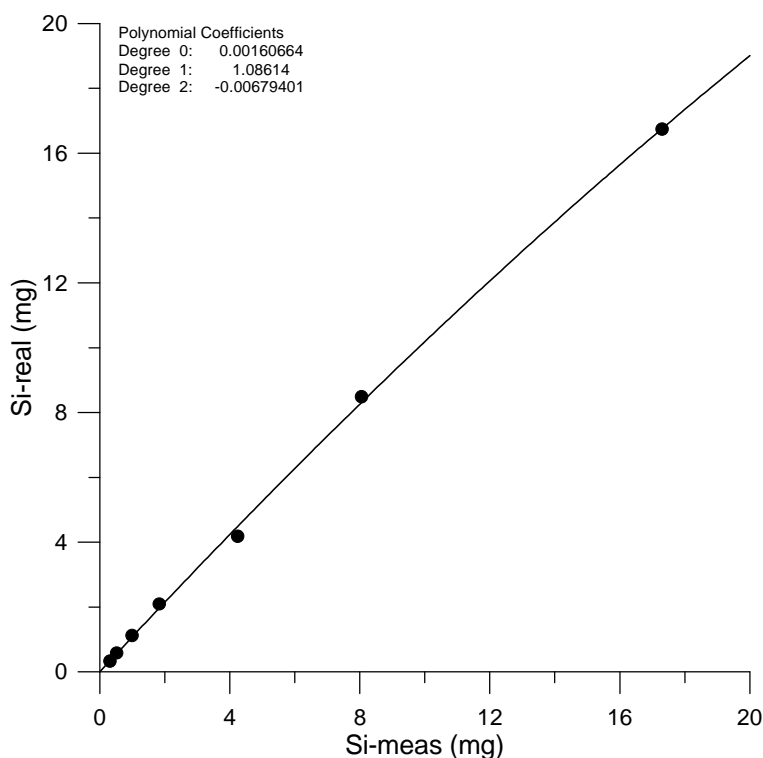
Typical calibration line for Si in MM91

Figure 2-A.2 A typical calibration line for the MM91 series. The known amount of Si is plotted against the measured Si content. From this calibration line, the final amounts of Si in the sediment trap samples are calculated from the measured amount of Si so as to avoid procedural artifacts.

Calculation of the mass accumulation rates

The calculation of the total mass on a filter was done in two ways: 1) by assuming a constant weight for each filter and subtracting this from the weights of the dried filter including the sample, and 2) by normalizing all elements to oxides (except Ca and Sr, which are normalized to carbonates). Both values appeared to agree well. The mass accumulation rates were then derived by multiplying with the split factor (4 for the first series, 8 for the remaining three) and by dividing with the number of collection days for each sample and the sediment trap aperture (1 m²).

Because the oxic sediment trap samples were too small to allow a separate analysis of biogenic Si (opal), clay-Si had to be calculated by assuming a constant Si/Al for clays of 2.6 (this value, corrected for the known quartz and opal content, is found in MM91, which consists of mixed eastern Mediterranean sediments). By multiplying the total accumulated Al by Si/Al_{clay}, clay-Si is then derived. This value is subtracted from total Si to give Si_{rest}, which consists of quartz and biogenic Si. Because these two cannot be separated, all Si_{rest} is assumed to be biogenic Si, which is an upper limit for the real value.